

Investigations on humic acid removal from water using surfactant-modified zeolite as adsorbent in a fixed-bed reactor

Awad F. Elsheikh¹ · Umi Kalthom Ahmad¹ · Zainab Ramli¹

Received: 27 March 2015 / Accepted: 8 December 2016 / Published online: 26 December 2016
© The Author(s) 2016. This article is published with open access at Springerlink.com

Abstract Natural organic matter (NOM) is ubiquitous in aquatic environments and has recently become an issue of worldwide concern in drinking water treatment. The major component of NOM is humic acids (HA). In this study, a natural zeolite (mordenite) was modified employing hexadecyltrimethylammonium bromide (HDTMA) to enhance greater efficient sites for sorption of HA. The natural zeolite and surfactant-modified zeolite (SMZ) were characterized by X-ray diffraction (XRD), Fourier-transform infrared spectrometer (FT-IR), N₂ Adsorption–desorption isotherms and BET-specific surface area, thermographic analysis, derivative thermographic analysis (TGA-DTA) and Field emission scanning electron microscopy (FESEM). A fixed-bed reactor was used for the removal of HA and the effects of different experimental parameters such as HDTMA loading levels, HA solution flow rate, solution pH and eluent concentration were investigated. The results indicated that the SMZ bed with HDTMA loading of 75% of external cation exchange capacity (ECEC) at a flow rate of 2 BV/h and pH of 10 showed the greatest enhanced removal efficiency of HA while ethanol solutions (25%v/v) with feed flow rate of 2 BV/h were sufficient for complete regeneration of SMZ and desorption of HA. Measurements of surface area of SMZ indicated

that a monolayer formation of the surfactant at those conditions allowed the optimum removal of HA.

Keywords Adsorption · Desorption · Humic acid removal · Surfactant-modified zeolite · Fixed-bed reactor

Introduction

Natural organic matter (NOM) which is ubiquitous in aquatic environments, ground and soil waters, has recently become an issue of worldwide concern in drinking water treatment (Rao et al. 2011). The major components of NOM are humic substances (HS) which are typically naturally occurring compounds that account for 30–80% of the dissolved organic matters in natural water (Yang et al. 2004). HS mainly consist of humic acid (HA), fulvic acid (FA), and humin (Matilainen et al. 2011). Since the early 1970s, water quality and treatment issues related to NOM have been reported, where these substances in natural water facilitated bacteria reproduction during drinking water distribution and produced harmful disinfection by-products (DBP), such as trihalomethanes (THMs), during chlorination process. They also caused a reduction in the effectiveness of water purification by interfering with various oxidants, increasing the solubility of heavy metals due to complexation with metals and adsorbed organic pollutants (Yang et al. 2007). Four main THM compounds are chloroform (CHCl₃), dichlorobromomethane (CHBrCl₂), dibromochloromethane (CHBr₂Cl) and bromoform (CHBr₃). They are classified as potentially carcinogenic chlorine organic compounds (Lee et al. 2009).

Numerous techniques have been used for the removal of NOM from sources of drinking water such as coagulation, flocculation, membrane filtration and advanced oxidation

✉ Umi Kalthom Ahmad
umikalthom@utm.my

Awad F. Elsheikh
awad2003@yahoo.com

Zainab Ramli
zainab@kimia.fs.utm.my

¹ Department of Chemistry, Faculty of Science, Universiti Teknologi Malaysia, UTM, 81310 Johor Bahru, Johor, Malaysia

processes (Wang et al. 2006). Among the techniques, adsorption is regarded as a promising method for the removal of HS from water. A variety of adsorbents such as amino-functionalized magnetic mesoporous silica, cationic surfactant-modified bentonite and activated carbon have been reported as being effective for the removal of NOM from drinking water (Dabrowski 1999). Consequently, it is very essential and important to explore adsorbents with a high adsorption capacity and efficiency to remove NOM from water.

Zeolites are crystalline aluminosilicates with a distinctive pore structure in the microporous range (Ismail et al. 2010). They are characterized by a large selectivity and the ability to separate substances based on the variation in sizes and shapes of separated molecules. As a result, the species with a molecular diameter which makes them too large to pass through a zeolite pore are effectively sieved. Adsorption processes derived from molecular sieving and selectivity are always reversible in theory and typically reversible in practice. This permits the zeolite to be reused many times, cycling between adsorption and desorption. This is one of the reasons for the substantial economic value of zeolites in adsorption applications.

Modification condition of the zeolites alters their pore structure permanently. The pore size reduction can be tuned by altering the modification circumstances. So as to manage the pore-opening size without affecting the internal pore systems of the zeolite, modification can be achieved using modifying agents with a molecular size larger than that of the zeolite pore so that they cannot enter them and they interact only with the external surface (surfactant zeolite).

Surfactants are widely used and have a very large number of applications due to their significant ability to influence the properties of surfaces and interfaces. In some usage, surfactants are defined as molecules capable of association to form micelles. These compounds are termed as surfactants, amphiphiles, surface-active agents, tensides, or, in the very old studies, paraffin-chain salts (Dabrowski 2001). Adsorption technologies have also been developed to overcome the deterioration of water quality (Wang and Peng 2010). The use of environmental friendly materials similar to zeolite as an adsorbent and water as a refrigerant makes this system very acceptable in many areas (Chen et al. 2011).

This work was aimed at finding the optimum conditions for the removal of HA from water using HDTMA as surfactant-modified zeolite (SMZ) and its desorption efficiency in a fixed-bed reactor. The SMZ was characterized by XRD analysis, FT-IR, N₂ adsorption–desorption isotherms and BET-specific surface area, TGA-DTA and FESEM micrographs and elemental analysis. The adsorption of HA on SMZ as a function of HDTMA loading

levels, feed flow rate and pH solution were observed using column experiments. Potential mechanisms for HA adsorption onto SMZ were also proposed.

Materials and methods

Chemicals and material

The natural zeolite (NZ) used in the experiments was supplied in Malaysia by Chan Chun Chan Enterprise Company. The NZ had the following total chemical compositions (in mass): SiO₂ 72.40%, Al₂O₃ 10.60%, Fe₂O₃ 2.00%, CaO 0.86%, MgO 1.83%, K₂O 2.15%, Na₂O 1.80%, TiO₂ 0.86%, a loss of ignition of 7.16% and pH of 9.10. The particle size of NZ was 425 μm with pore diameter of 65.32 Å. In consistent with the reported methods (Childs 1994), the cation exchange capacity (CEC) of NZ was determined to be 1.083 meq/g and the ECEC was 45.6 meq/100 g. The reagents used for cation exchange capacity (CEC) were sodium acetate (NaOAc), ammonium acetate (NH₄OAc) and isopropyl alcohol supplied by QRëC, Malaysia. HA was produced by Fluka, Switzerland. Sodium acetate (NaOAc), glacial acetic acid (99.5%), concentrated ammonium hydroxide (NH₄OH) and hexadecyltrimethyl ammonium bromide (HDTMA) were supplied by Molekula, UK.

Characterization

NZ and SMZ were subjected to several instrumental characterizations. Flame photometer model PFP7 from JENWAY, (UK), was used to determine CEC of elements for NZ. A Perkin-Elmer UV-Vis spectrophotometer (Lambda 25, USA) was used to determine HA concentration. The XRD pattern was recorded with a CuK α radiation ($\lambda = 1.5418$) at 30 kV and 20 mA ranging from $2\theta = 5^\circ$ to 50° and scanning speed of 0.05° per second in a Siemens D5000 X-Ray Diffractometer (Karlsruhe, Germany). The BET method used a single-point surface area to determine the surface area of NZ and SMZ employing the BET Micromeritics Pulse Chemisorb 2705 (Atlanta, USA) at 77 K with gas composition of 30% N₂ and 70% He. FT-IR of NZ and SMZ were recorded in the range of 400–4000 cm⁻¹ using a Perkin-Elmer Spectrum TM 400 FTIR spectrometer (Waltham, MA, USA). The surface of NZ and SMZ was examined by FESEM and EDX experiments using a Carl Zeiss Model Supra 35-VP FESEM (Oberkochen, Germany). The samples were gold coated to avoid electrostatic charging during examination and it was operated at 10 kV, Mag 75.00 kx and WD 8 mm. Energy dispersive X-ray (EDX) analysis system (EDAX Falcon System) was employed to analyze the presence of elements

in the specimens that have been sputtered with gold. TGA and DTA of NZ and SMZ samples were conducted using a Pyris Diamond Perkin-Elmer (Yokohamo-shi, Japan). The samples (9.562–12.950 mg) were heated from 50 to 1000 °C at a heating rate of 10 °C/min under a nitrogen flow rate of 100 mL/min and held for 10 min at 1000 °C.

Preparation of surfactant-modified zeolite

The surfactant modified zeolites (SMZ) were prepared by mixing 10 g of NZ with varying amounts of HDTMA aqueous solutions in 200 mL distilled water placed in a 400 mL flask. The mixture was then shaken at 150 rpm for 8 h. HDTMA loading levels ranged from 0 to 200% ECEC of zeolite (SMZ-0% to SMZ-200%). The samples were then filtered, washed with distilled water and dried at 70 °C in an oven for 3 h (Wang et al. 2006). Subsequently, the dried SMZ was then crushed by passing it through standard ASTM sieves yielding a particle size of 425 µm of all samples.

Adsorption

The laboratory-scale experimental setup was as described in an earlier reported study (Elsheikh et al. 2015) except with an additional ethanol solution tank. Experiments were performed to determine the optimal loading level of HDTMA for preparing modified zeolite for subsequent removal of HA by SMZ in the column system. The system consisted of a fixed-bed column to which HA solution was pumped from the HA solution tank to the bottom of the column; the temperature of the solution was controlled at (25 ± 0.5) °C. In the first stage of the experiment, a peristaltic pump MASTER FL 77240-10 was used to feed the HA solution (6 mg/L) to the bed filled with SMZ with HDTMA loading of 0, 50, 75, 100, 125, 150 and 200% of ECEC at a flow rate (Q) of 2 BV/h, respectively. The bed volumes (BV) of column were calculated using Eq. (1) as follows (Wang et al. 2006):

$$BV = \frac{V_H}{V_R} \quad (1)$$

where V_H is total HA solution volume passing through the column during the adsorption (mL). V_R is fixed-bed volume (mL). In the second stage, the HDTMA loading level was determined and the optimal flow rate and solution were examined. The HA solution was introduced into the column at a flow rate (Q) of 2, 3, 5BV/h and pH 4, 7, 10, respectively. Samples were collected and analyzed against percent loading of SMZ for HA solutions. The collected effluent was centrifuged, and the residual concentration of HA was measured using a UV–Vis

spectrophotometer at a wavelength of 254 nm. The adsorption capacity model (A_{ad}) for NZ and SMZ was calculated using Eq. (2) as follows (Lin and Zhan 2012):

$$A_{ad}(\text{mg/g}) = \frac{(C_i - C_e)V_H}{M} \quad (2)$$

where C_i is the HA concentration in the influent (ppm), C_e is the HA concentration in the effluent (ppm), and M is the mass of adsorbent (g). The collected HA was calculated from the difference between influent and effluent concentrations and bed volumes. The HA removal efficiency was calculated using Eq. (3) (Lin and Zhan 2012):

$$\text{Removal efficiency (\%)} = \frac{C_i - C_e}{C_i} \times 100 \quad (3)$$

Desorption

Regeneration of SMZ and desorption of HA was examined by eluting the HA using ethanol as eluent. For desorption experiments, HA was initially adsorbed at the optimum HDTMA loading level. After adsorption, ethanol solution (5, 10, 15, 20 and 25 percent volume, respectively) was pumped from the ethanol solution tank to the bottom of the column to elute the HA at the optimal flow rate of adsorption (2 BV/h). In every step, samples from the effluent were collected and analyzed using a UV–Vis spectrophotometer at a wavelength of 254 nm. Afterwards, the efficiency of the regenerated SMZ was studied in the three cycles of adsorption, desorption and resorption for HA removal. Every cycle was conducted at the obtained optimal conditions. The breakthrough curves of HA removal were constructed by linking the results of effluent concentration to the percentage of ethanol concentration from the above processes to obtain the desorption efficiency. Desorption efficiency defined as the ratio between the adsorption capacity of HA desorption (A_{de}) and the adsorption capacity of HA adsorbed on adsorbent (A_{ad}) was calculated as in Eq. 4 (Lin and Zhan 2012):

$$\text{Desorption efficiency (\%)} = \frac{A_{de}}{A_{ad}} \times 100 \quad (4)$$

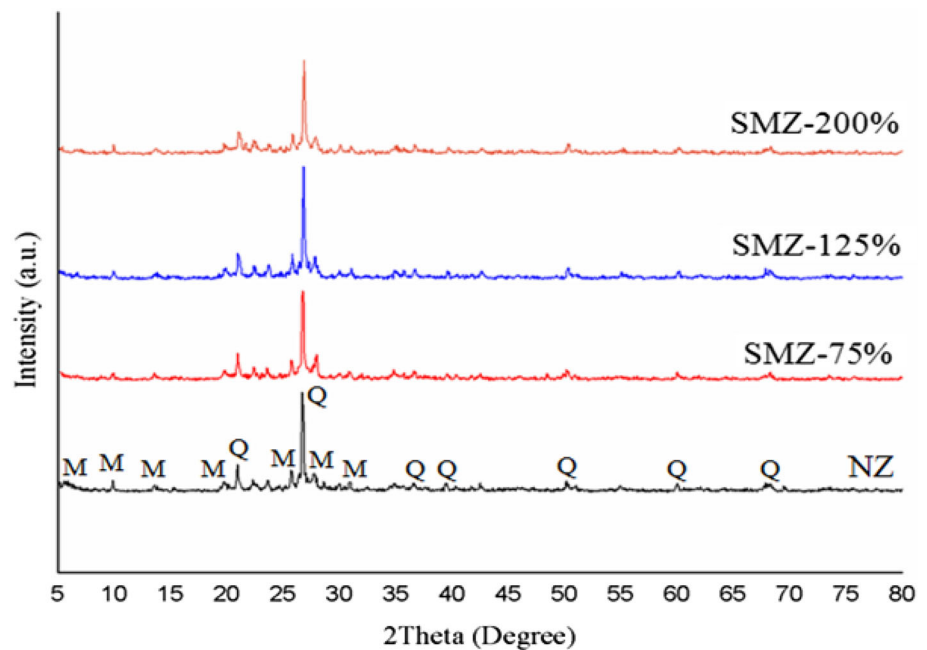
Results and discussion

Characterization

XRD analysis

NZ sample may include a diversity of other minerals such as quartz, montmorillonite and feldspar (Castaldi

Fig. 1 XRD pattern of NZ and SMZ, where M denotes mordenite and Q denotes quartz



et al. 2008). Figure 1 shows the X-ray diffraction (XRD) patterns of the natural zeolite (NZ) and SMZ at different loadings of HDTMA. The minerals that exist in the zeolite material are specified by comparing the characteristic peaks shown in the XRD pattern with the diffractometer database. Numerous peaks corresponding to minerals mordenite (M) and quartz (Q) have been identified in the XRD patterns of the zeolite. The model unit cell formula of NZ mineral, mordenite, is given as $\text{Na}_8 [(\text{Al}_2\text{O}_3)_4 (\text{SiO}_2)_{40}] \cdot 24\text{H}_2\text{O}$. This demonstrates a silica/alumina ratio of 10:1 (Bajpai 1986). Quartz was detected as a major component in the NZ with 78.13% while mordenite gave only 21.86% based on the percentage of peak intensity at I_{100} for mordenite and I_{100} for quartz (Fig. 1). Its crystal structure (i.e. quartz) is a continuous framework of SiO_4 silicon–oxygen tetrahedral. The high silica content of NZs produces high Si/Al ratios which lead to excellent hydrophobicity. The XRD profiles of the different loading capacity of HDTMA-modified zeolites (SMZ-HDTMA) are very similar to those of the corresponding parent NZ; this indicates that the crystallinity of the NZ remained intact after chemical treatment with HDTMA molecules. The relative intensity (I_{rel}) of the X-ray peaks corresponding to some typical crystallographic planes of the NZ and SMZ is presented in Table 1. The relative intensity of the mordenite characteristic peaks was at 2θ of 9.87° , 13.58° , 19.74° , 22.29° , 25.73° , 26.71° , 27.70° , 29.98° and 30.92° , which increased due to the cation exchange reaction that took place in NZ when they were modified by HDTMA.

Fourier-transform infrared spectroscopy

FTIR spectra of the NZ, HDTMA and SMZ are shown in Fig. 2. The band observed at 3425 cm^{-1} is assigned to hydroxyl group of water. For the structure of zeolite T–O, asymmetric and symmetric stretching of T–O (T=Si or Al) is observed between 998 and 665 cm^{-1} . Band at 553 cm^{-1} is assigned for double six rings for Si–O–T bonds of zeolite framework while band at 461 cm^{-1} is assigned for bending is assigned for bending mode of T–O (Elaiopoulos et al. 2010). The presence of additional peaks at 2918 – 2841 cm^{-1} is caused by C–H stretching of hydrocarbon originating from the HDTMA which is present in the SMZ structure. The frequencies and widths of the CH_2 stretching modes depend strongly on the conformation and the packing density of methylene chains (Rozic et al. 2009). Broadening of bands in SMZs implied that HDTMA molecules on the modified zeolites have a more disordered structure than the NZ.

N_2 adsorption–desorption isotherms and BET-specific surface area

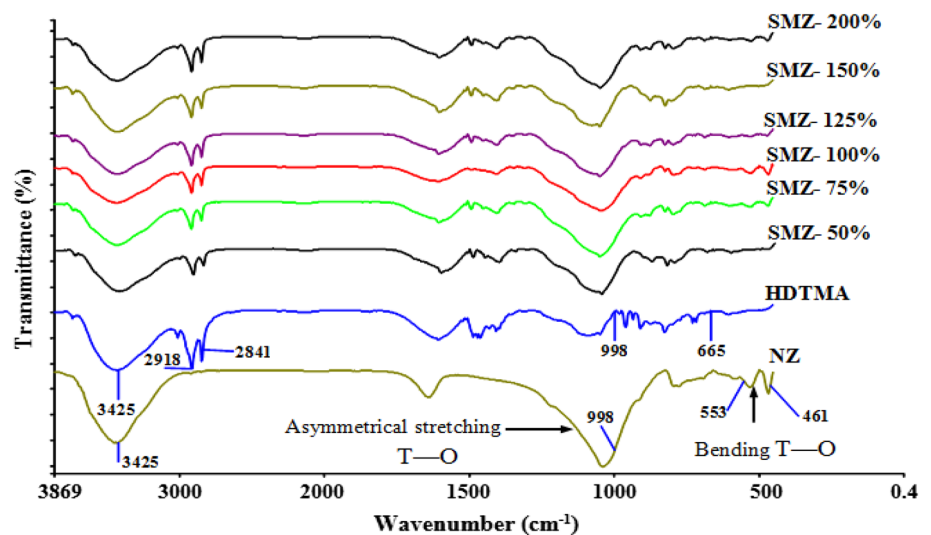
Figure 3 shows the N_2 adsorption–desorption isotherms of NZ and SMZ-75%. Both NZ and SMZ-75% showed a type IV adsorption isotherm with an obvious hysteresis loop, signifying the presence of mesopores in both samples (Zhang et al. 2012). The isotherm for NZ showed an obvious and light wide hysteresis loop at relative pressures of ca. 0.45, which is distinctive for mesoporous zeolite of ink-bottle type pores with pore necks lesser than 4 nm (Fig. 3a) (Qin et al. 2011). After

Table 1 Typical X-ray peaks of natural zeolite

2θ	NZ		SMZ-50%		SMZ-75%		SMZ-200%	
	d (Å)	I_{rel}	d (Å)	I_{rel}	d (Å)	I_{rel}	d (Å)	I_{rel}
9.87	8.95	10.4	8.90	9.3	8.98	7.9	9.02	11.1
13.58	6.51	6.1	6.56	9.3	6.57	5.4	6.52	7.1
19.74	4.49	9.7	4.48	12.1	4.49	10.7	4.50	10.5
22.29	3.98	12.8	3.97	15.7	3.97	12.7	3.98	16.2
25.73	3.45	22.4	3.46	23.1	3.46	23.1	3.46	23.0
26.71	3.33	100.0	3.33	100.0	3.33	100.0	296	100.0
27.70	3.21	18.0	3.21	26.0	3.21	20.0	3.21	20.3
29.98	2.97	7.7	2.98	8.9	2.98	8.5	2.98	11.5
30.92	2.88	10.1	2.89	11.0	2.88	10.4	2.89	9.8

d , interplanar spacing; $I_{rel} = I/I_{max}$, relative intensity

Fig. 2 FTIR spectra of natural zeolite, HDTMA and SMZ (T = Si or Al)



modification, the vertical hysteresis loop of SMZ-75% was closed for $P/P_0 = 0.40$ which indicates the presence of mesopores volumes in SMZ-75% and suggested the presence of cylindrical type pores (Fig. 3b).

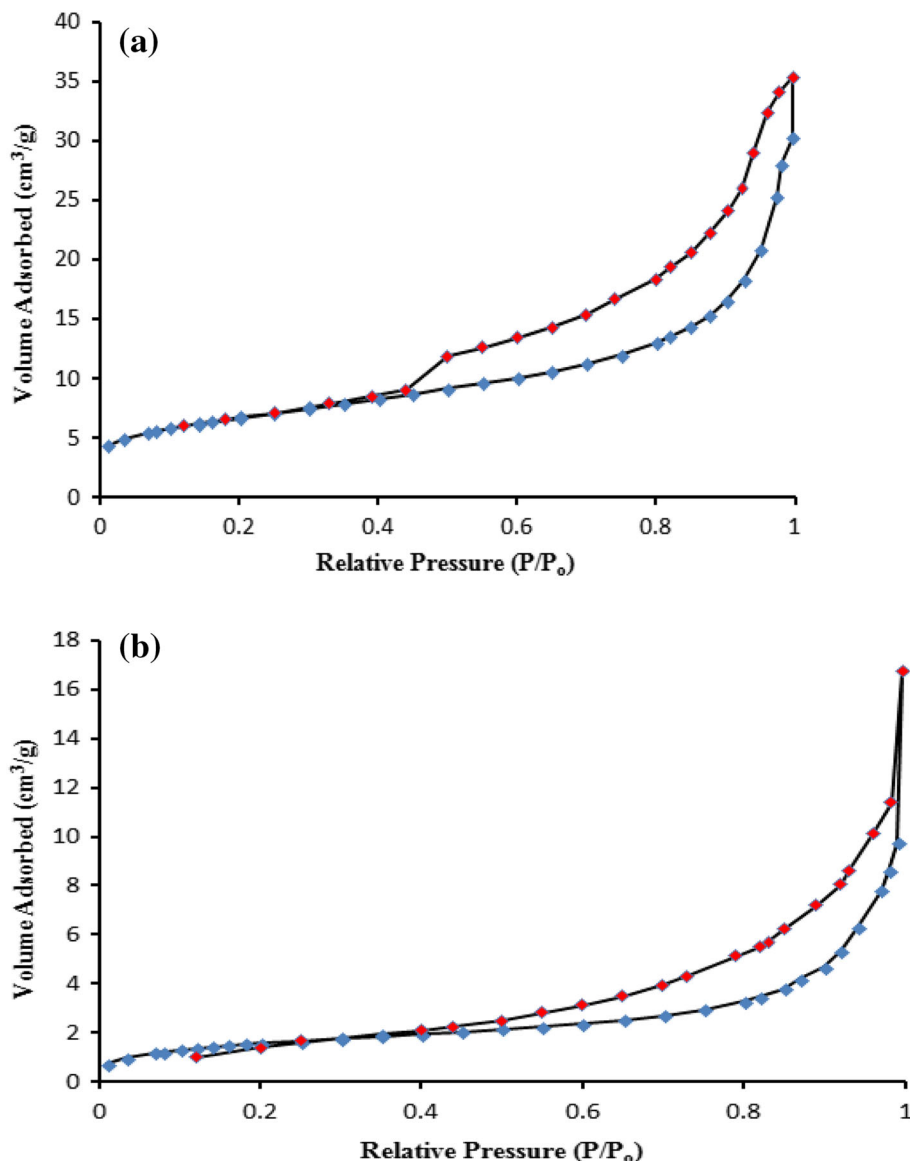
The BET surface area of NZ was $23.99 \text{ m}^2/\text{g}$ while SMZ-75% was $11.83 \text{ m}^2/\text{g}$. The total pore volumes of NZ and SMZ-75% were found to be 0.039 and $0.026 \text{ cm}^3/\text{g}$, respectively. It was evident that the surface areas and pore volumes of NZ have decreased significantly after the modification with the cationic surfactant HDTMA. This is due to the presence of HDTMA molecules on the zeolite surface which hampered some of the main pore channels of NZ, thus obstructing the diffusion of N_2 throughout these channels (Leyva-Ramos et al. 2008). The surface area measurement for adsorption capacity is important for the HA removal efficiency. In general, a larger surface area translates into a greater adsorption capacity.

Figure 4 illustrates the effect of HDTMA loading levels on zeolite surface area and the HA removal

efficiency. Surface area changes with different HDTMA loadings to reflect the transition between monolayer and bilayer coverage of HDTMA on the SMZ. HA removal efficiency is at maximum when the SMZ has the highest surface area at 75% HDTMA loading level on the NZ (SMZ-75%). The result showed that HA removal efficiency increased gradually (submonolayer) with increasing HDTMA loading level until SMZ-75% (monolayer) which is the maximum removal efficiency (Fig. 4). Also, the HDTMA-modified zeolite with higher surfactant loading amounts (SMZ-200%) exhibited a worse HA adsorption capacity. This is due to the formation of bilayer of HDTMA which decreases the surface area and reduces the interparallel pore size (Wang et al. 2006).

Figure 5 shows the proposed schematic diagram of adsorbed surfactant molecules (HDTMA) on the surface of the zeolite. The surface increasingly mislays its negative charge with rising HDTMA loading and becomes more

Fig. 3 N₂ Adsorption–Desorption Isotherms for **a** NZ, **b** SMZ-75%



hydrophobic. With decreasing surface area, the interparallel pore size increases from 65.32 Å for NZ to 86.17 Å for SMZ-75%, thus the ability to sorption more HDTMA increases and, thus, more adsorption for HA (Fig. 5b). The zero point of charge (zpc) refers to the point of equilibrium between loading of HDTMA and adsorption of the largest amount of HA, SMZ-75% (Wang et al. 2006). For submonolayer sorption of SMZ-50%, the distribution and, hence, the density of HDTMA in the NZ are controlled by the charge on the zeolite surface as schematically shown in Fig. 5a. HDTMA, a high-molecular weight surfactant (402.46 g/mol), is too large to enter the internal micropores of zeolite channels and, thus, is only able to access the external surface area. Figure 5b also shows that at SMZ-75%, the negatively charged zeolite surfaces are covered by HDTMA and form monolayers of HDTMA. At this

stage, SMZ-75% is mostly hydrophobic. The zpc at SMZ-75% may correspond to a complete monolayer surface coverage by HDTMA, which means that it is a good indicator for a surface exhibiting maximum hydrophobicity (Fig. 5b) that leads to the maximum adsorption efficiency of HA. At values higher than the zpc (Fig. 5c), another layer of HDTMA molecules decreases the surface area and changes the surface charge. As a result, interparticle size becomes smaller for the HA to enter and be adsorbed (Wang et al. 2006) and once more, the surface becomes hydrophilic.

On the other hand, a common pattern of cationic surfactant loading on the zeolite surface is the formation of a monolayer or “hemimicelle” at the solid–aqueous interface by a cationic exchange process at surfactant concentration at or below its critical micelle concentration (CMC).

Fig. 4 Effect of HDTMA loading levels on zeolite surface area and removal efficiency of HA

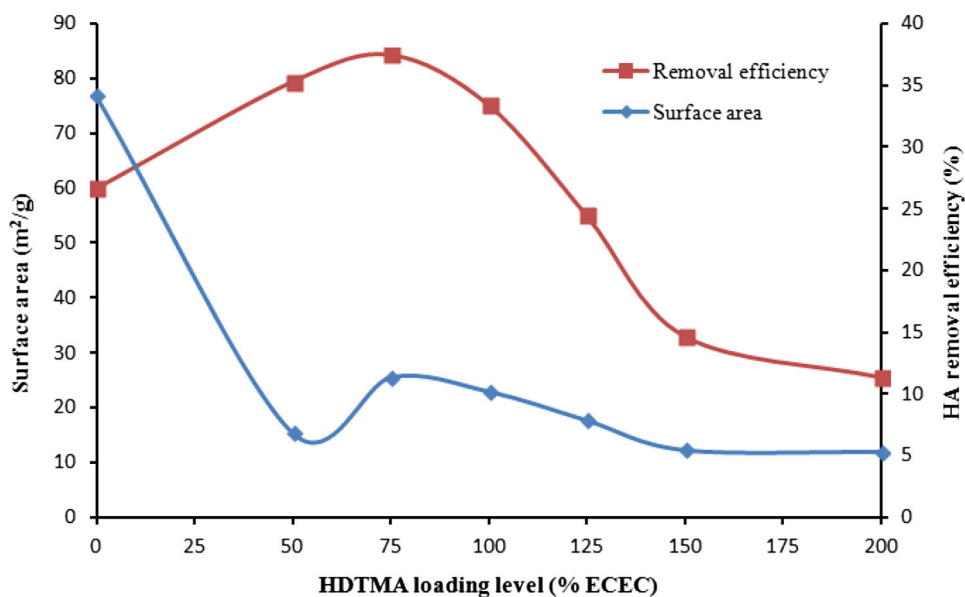
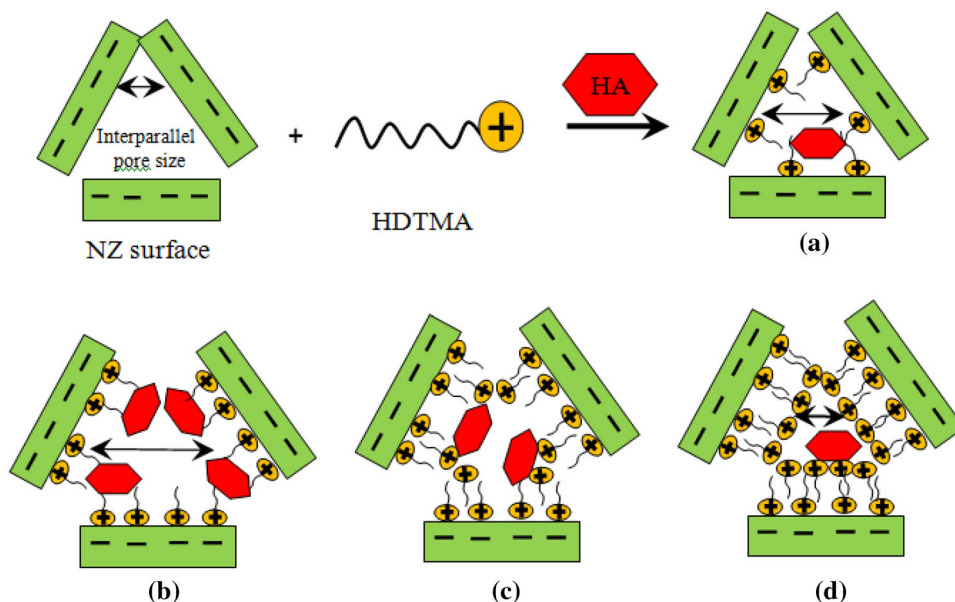


Fig. 5 Schematic diagrams of HDTMA configurations on the zeolite surface. **a** SMZ-50%, **b** SMZ-75% (below CMC), **c** SMZ-150% and **d** SMZ-200%, HDTMA in a bilayer (above CMC)



While aqueous cationic surfactant concentration is larger than the CMC and sufficient amount of surfactant exists in the solution, the loaded cationic surfactants on the external surface of the zeolites form a bilayer (above CMC) (Li et al. 2000). The optimum amount of HDTMA occurred at the loading level of 75% ECEC in which the HDTMA is expected to form a monolayer on the external surface of the zeolite with the lower surface held by the electrostatic attraction between the negatively charged zeolite surface and the positively charged HDTMA head groups as in Fig. 5b. The upper surface is connected to the lower surface through the hydrophobic interaction between the HDTMA and tail groups in both surfaces as shown in Fig. 5d (Zhan et al. 2010).

Thermal analysis

Weight loss due to thermal treatment in the NZ and SMZ samples is presented in Fig. 6 and the amount of the weight loss is given in Table 2. The TGA curve for NZ is shown in Fig. 6a. There are three stages of weight loss observed. The external water was released up to 250 °C followed by loosely bound water where it was lost rapidly up to 275 °C. After 275 °C, the NZ started to lose its tightly bound water (Lin and Zhan 2012). The average percent weight loss up to 700 °C was calculated as 21.47%. Three intensive derivative curve peaks due to the loss of water molecules were observed from DTA at 70, 260 and 425 °C. The TGA curve for SMZ-75% is shown in Fig. 6b. Four stages of

Fig. 6 TGA results for **a** NZ, **b** SMZ-75%, **c** SMZ-200%

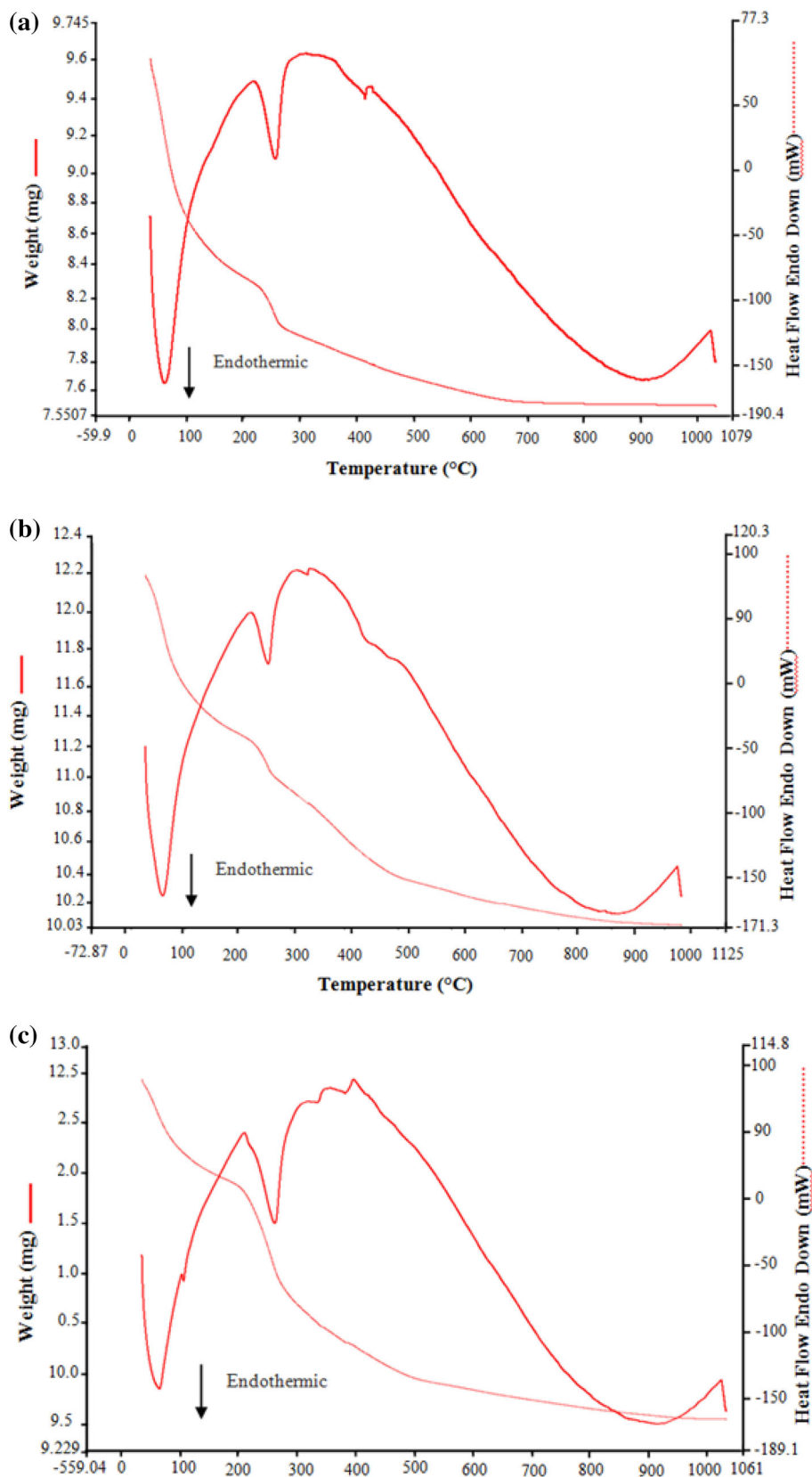


Table 2 The percentage weight loss of external, loosely bound and tightly bound water for NZ, SMZ-75% and SMZ-200%

Sample Temperature	EW (%) (150 °C)	LBW (%) (150–300 °C)	TBW (%) (300–500 °C)	OM (%) (500–700 °C)	TBW (%) (>700 °C)	Total (%)
NZ	13.20	2.62	3.66	0.00	1.99	21.47
SMZ-75%	8.91	1.61	4.83	2.02	1.78	19.15
SMZ-200%	9.27	5.79	6.95	2.32	4.40	28.73

EW external water, LBW loosely bound water, TBW tightly bound water, OM organic material

weight loss were observed. The weight loss below 500 °C was mainly attributed to the external, loosely and tightly bound water. The weight loss between 500 and 700 °C was mainly attributed to the decomposition of HDTMA within the SMZ-75%. The total weight losses as a result of the degradation of HDTMA and water molecules were found to be about 19.15%. The total weight loss of external water and loosely bound water for SMZ-75% was lower than that of NZ, confirming the loading of HDTMA onto zeolite. For sample SMZ-200% (Fig. 6c), two intensive derivative curve peaks were observed where the HDTMA covers some zeolite pore. The decomposition of HDTMA within SMZ takes place in two phases; the first phase was attributed to the decomposition of surfactants bound to their adjoining molecules through hydrophobic interaction, while the second phase was due to the loss of surfactants bound to the surface of the zeolite through electrostatic interaction (Lin and Zhan 2012).

The occurrence of the derivative curve peak between 500 and 700 °C in the SMZ DTA curve, which was missing in the NZ DTA curve, confirmed that some HDTMA molecules had been bound to the zeolite surface via electrostatic interaction after the modification process. The weight loss between 500 and 700 °C for SMZ-200% was much higher than that for SMZ-75%. The suggested bilayer of HDTMA bound on the NZ surface was confirmed by Fig. 5d. Moreover, the results from Table 2 shows that NZ are hydrophilic materials where the total weight lost is higher (21.47%) due to water molecules loss compared to SMZ-75% (17.13%). This was due to the formation of the monolayer of HDTMA that changed into hydrophobic layer as illustrated in Fig. 5b. With the increased loading of HDTMA as in SMZ-200%, the total weight loss by water molecules increased (24.33%) due to the bilayer formation when the surface became hydrophilic again, and hence becoming increasingly prone to attracting water (Fig. 5d) (Kim and Ahn 2011).

FESEM micrographs and elemental analysis

The morphologies of the NZ and SMZ-75% were captured using FESEM. The great difference in the surface

morphology was observed. Figure 7a shows a distinct flowery pattern with some sheet-like morphology for natural zeolite. On the other hand, the SMZ-75% illustrates an image of a smooth surface (Fig. 7b). This result shows that an organic layer was formed on the surface of natural zeolite after being modified by HDTMA.

EDX is a surface analytical technique and the results of EDX elemental analysis are presented in Table 3. Since energy dispersive is less sensitive to elements with atomic numbers less than 20, the percentage weight listed in the related tables in these figures has been calculated on an oxygen-free basis (Shams and Mirmohammadi 2007). EDX is a surface analytical technique. The elemental compositions obtained indicate that the elemental weight percentages of carbon ions increased from near zero in NZ to 10.81% in SMZ-75%, which indicates the presence of HDTMA. On the other hand, the elemental weight percentages of potassium and iron ions decreased, which shows that ion exchange occurred for K^+ , Mg^{++} , Fe^{++} and Na^+ . The percentage of Na^+ in the EDX spectrum of sample NZ is low. Sodium ions included within the interparallel pore are more difficult to recover by ion exchange (Shams and Ahi 2013). The larger pore size of SMZ (86.17Å) provides a more facile passage for metal ions and increases its resulting exchange rate rather than NZ (65.40Å). The modification of NZ by HDTMA results in an increased the interparallel pore size and decreased surface area.

The NZs with high Si/Al ratio have long been recognized to possess hydrophobic properties. The degree of hydrophobicity is normally dependent on the Si/Al ratio (Hsu and Ma 1988). Olson et al. (1980) illustrated that the amount of water adsorbed decreases linearly with an increase in Si/Al ratio. In this study, the EDX and also XRD results show that the NZ has a high percentage of quartz (Si) that affects the Si/Al ratio and increased from 3.47 to 5.04% after modification. This result indicates that the NZ has changed from hydrophilic to hydrophobic.

Fig. 7 FESEM photographs **a** NZ; **b** SMZ-75% at 10.00 KX magnifications

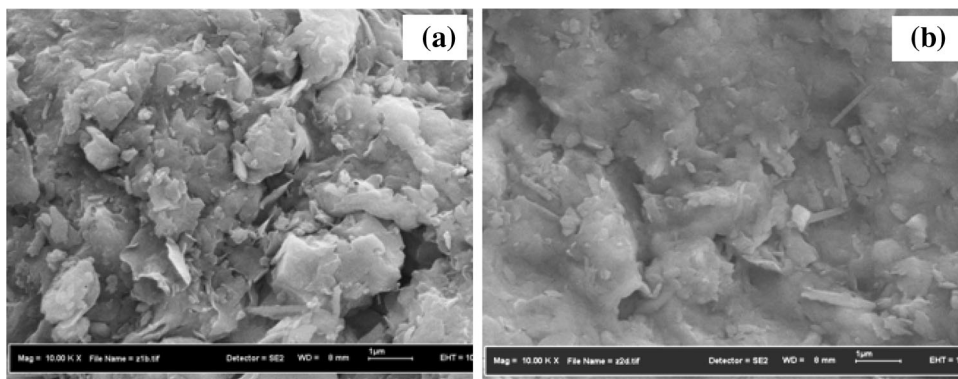


Table 3 EDX elemental analysis of NZ and SMZ-75%

Element	NZ (wt%)	SMZ-75%
C	0.00	10.81
Na	0.29	0.41
Si	28.45	32.98
Al	8.21	6.55
Mg	1.11	0.31
K	4.58	1.97
Fe	3.30	0.99
Si/Al	3.47	5.04

Adsorption

Effect of HDTMA loading levels

The removal of HA by SMZ samples at 0–200% HDTMA loading was performed at various flow rates, as presented in Fig. 8. It was found that the most optimal removal of HA occurred at HDTMA loading of 75% ECEC (SMZ-75%) at an optimum flow rate of 2 BV/h. As shown in Fig. 9, the removal efficiency (%) and adsorption capacity of SMZ are

highest for SMZ-75%, i.e. almost 90% higher than that of NZ (59%). It was also found that the adsorption capacity is approximately 1½ times higher than that of natural zeolite.

The major mechanisms involved are the physical and chemical adsorption of HA to SMZ. The NZs contain only micropores and external surface area, but after modifications, a mesoporous structure could be shaped (Rozić et al. 2009). The adsorption mechanisms are as follows: anion/cation exchange, cation exchange, van der Waals interactions, hydrogen bonding, hydrophobic effects and ligand exchange (Wang et al. 2006). A complete organic monolayer surface coverage by HDTMA means that electrostatic interaction, ligand exchange and cation bridging could not be the dominant mechanism. Hydrophobic interaction and hydrogen bonding are possibly the main mechanism in HA adsorption by SMZ. In adsorption by NZ, the HDTMA loading level of 0 percent is relatively unimportant perhaps because of the intense dipole interaction between zeolite and water, which keep out the NOM from the zeolite (Zhan et al. 2010). The result showed that NZ had an insignificant attraction for HA in water.

After NZ was modified with HDTMA, the resulting hydrophobic organic monolayer surface would induce more contact and interaction with soluble HA, in turn

Fig. 8 Effect of HDTMA loading on concentration of HA at various feed flow rates ($C_i = 6$ mg/L; solution pH = 7.0)

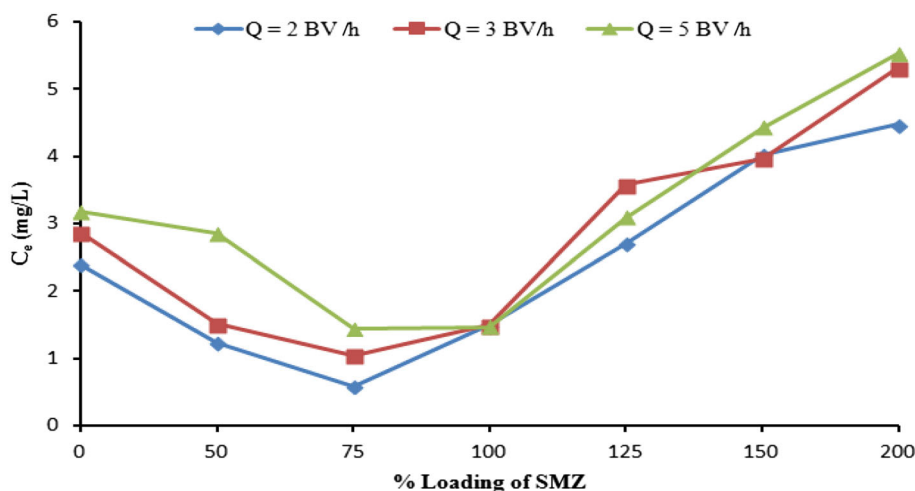
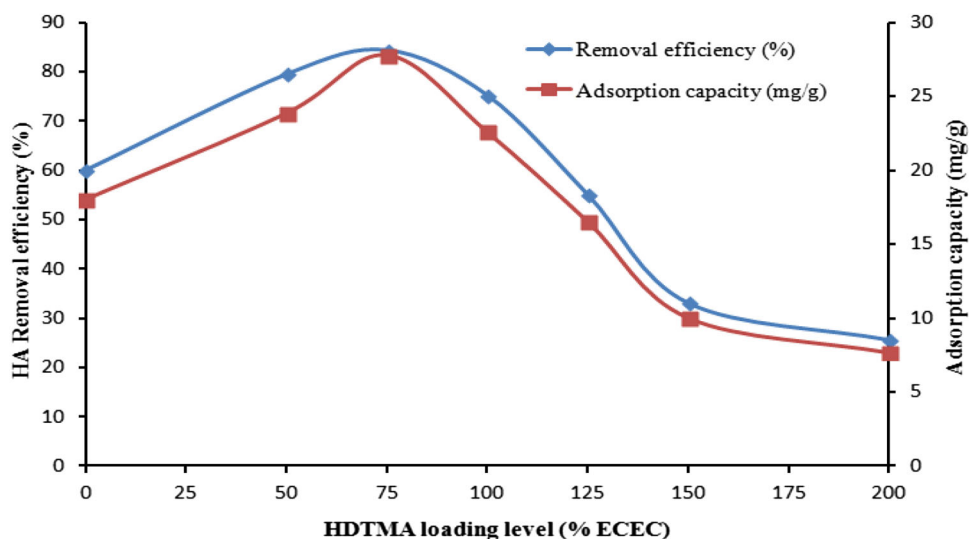


Fig. 9 Effect of HDTMA loading as SMZ on HA adsorption ($C_i = 6$ mg/L; $Q = 2$ BV/h; solution pH = 7.0)



improving the adsorption of HA by van der Waals interactions (Fig. 5a). The high number of hydrogen bonds between C or N of HDTMA and hydroxyl groups, carboxylic groups and phenolic groups of HA guarantees more effective adsorption of HA. At SMZ-75%, maximum hydrophobicity encourages higher contact and interaction, so SMZ favors a large amount of removal of HA at this point (Wang et al. 2006). Hydrogen bonds also exist among the functional groups of HA. The amount of interparallel pores size at this point makes it possible for a higher adsorption rate of HA molecules (Fig. 5b). Other than the above SMZ-75%, a compact effective volume also causes a lower adsorption (Fig. 5d). This adsorption behavior may reveal why the best performance occurred at the SMZ-75%.

Effect of feed flow rate

The results of bed volume at different flow rates were determined at SMZ-75%. The breakthrough curves were obtained by plotting HA concentrations in the effluent versus feed flow rates as presented in Fig. 8. The breakthrough point in the system occurred at SMZ-75% for flow rates (Q) of 2, 3 and 5 BV/h. The minimum feed flow rate facilitates more effective elimination of HA compared to higher flow rates due to the higher contact time at low flow rate, which ensures sufficient mass transfer. Weak distribution of the HA inside the column leads to a minimized diffusivity of the HA solution among SMZ particles.

Effect of solution pH

The effect of solution pH on HA adsorption onto SMZ was studied. The breakthrough curves at different pH (4, 7 and 10) are shown in Fig. 10. It is clear that pH plays a large

role for the adsorption of HA (Wang and Peng 2010). Figure 10 indicates the behavior of HA adsorption onto SMZ as a function of pH, exhibiting a higher uptake of HA which occurred at a pH of 10.00. The decrease in the solution pH resulted in different passive effects on HA adsorption efficiency. At initial HA solution concentration of 6 mg/L, a decrease of solution pH from 10 to 4 leads to decreased total HA removal efficiency of adsorbent. The HA adsorption mechanisms by SMZ are mainly related to the charge and the structural morphology of HA molecule and zeolite framework structure at different solution pH (Roger et al. 2010). HA is a mixture of organic compounds with weakly acidic functional groups, such as carboxylic and phenolic groups. The charge of HA molecules changes with pH because the pKa values of carboxylic and phenolic groups are about 3.0 and 9.0. HA is probably negatively charged with increased pH by deprotonation of carboxylic groups, resulting in the more HA adsorption capacity. Carboxylic and phenolic groups have an important role in the charge of HA molecules. The dissociation of carboxylic groups occurs at pH more than 4, while the phenolic groups are subjected to dissociation at pH more than 8. For this reason, with increasing influent pH, the negatively charged HA molecules increase by increasing deprotonation of the carboxylic groups (Mohd Omar et al. 2014; Lin and Zhan 2012).

Desorption of HA

The regeneration of SMZ and desorption of HA were affected in the SMZ bed with SMZ-75% at a feed flow rate of 2 BV/h. 0.45 mg/L HA influent concentration was obtained at 75 BV for feed flow rate of 2 BV/h. The optimum SMZ regeneration was obtained at an ethanol solution concentration of 25% volume with a feed flow rate

Fig. 10 Effect of solution pH on HA adsorption ($C_i = 6$ mg/L; $Q = 2$ BV/h)

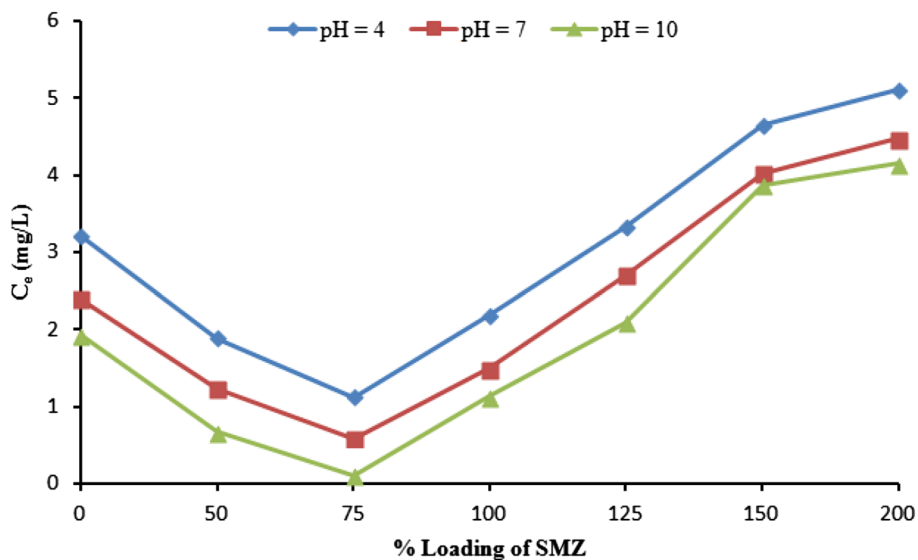


Fig. 11 Adsorption of HA by SMZ-75% and regenerated SMZ-75% at different ethanol concentration ($C_i = 6$ mg/L, $Q = 2$ BV/h)

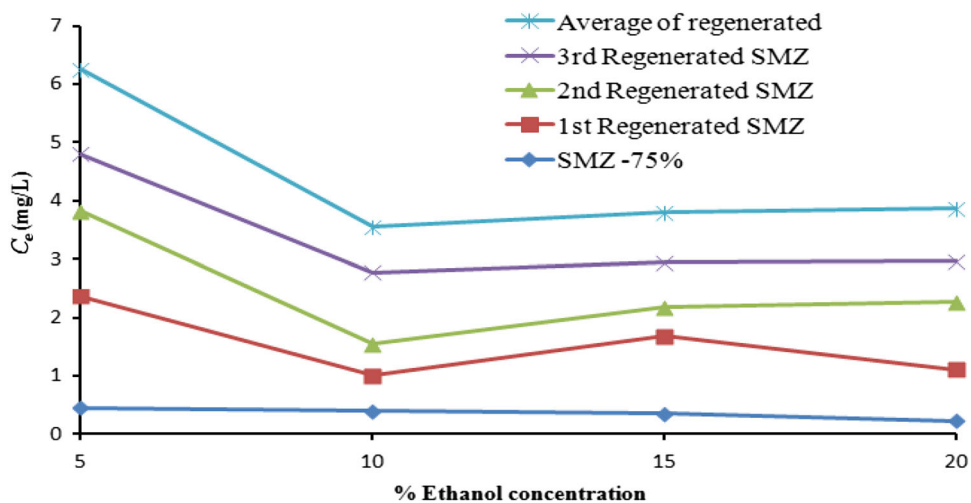
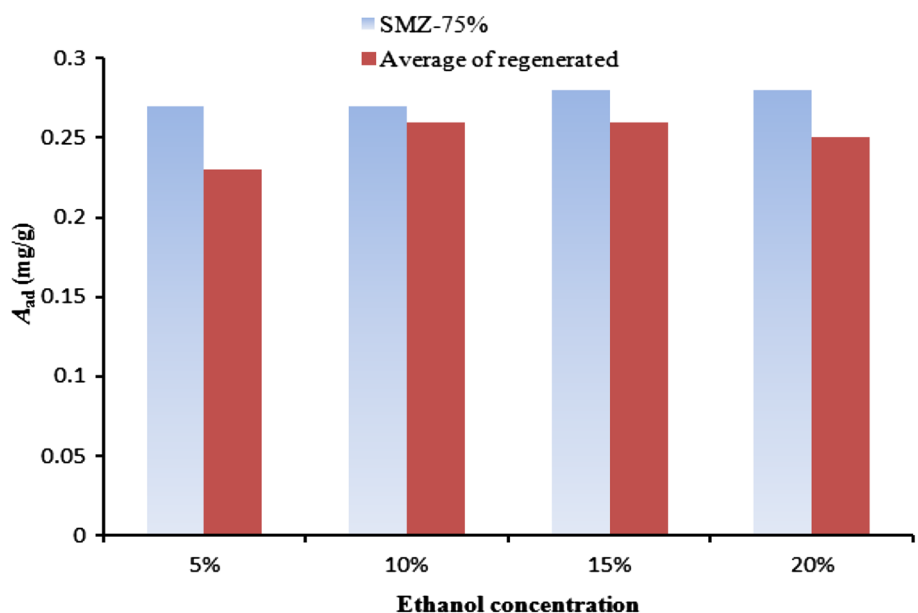


Fig. 12 Adsorption capacity of HA by SMZ-75% and regenerated SMZ-75% at different ethanol concentration ($C_i = 6$ mg/L, $Q = 2$ BV/h)



of 2 BV/h. With an optimum parameter of 25% volume of regeneration solution, it was sufficient to reduce HA concentration in regeneration solution effluent to less than 0.6 mg/L of HA. Figure 11 represents the adsorption of HA by SMZ-75% and by regenerated SMZ-75%. The breakthrough point of effluent concentration is at 0.44 mg/L for SMZ-75%; meanwhile, the breakthrough points are 1.02, 0.42 and 0.30 mg/L for regenerated SMZ in the 1st, 2nd and 3rd cycles, respectively. As observed from Fig. 12, there is an average of 3.57% loss of adsorption capacity after regeneration. The adsorption capacity for SMZ and regenerated SMZ in the first cycles was found to be 28 and 27 mg/g, respectively. The curves of regenerated SMZ-75% in three cycles are very comparable, which exemplify that the same regeneration effect and long-term stability can be acquired.

Desorption is produced by the formation of hydrogen bonding between the hydroxyl group of ethanol and the function groups of HA (Lin and Zhan 2012). When the concentration of ethanol increases to a sufficient value, the hydrogen bonding would be stronger than interactions of adsorption and the adsorbed HA could be eluted. But at lower concentration of ethanol, less contact is made between HA and the eluant. At higher concentration of ethanol, there is a higher efficiency of desorption due to the incapability to efficiently interact with HA molecules that contain numerous functional groups.

Conclusions

The surface of natural zeolite was modified with HDTMA to enhance its HA adsorption capability. The HDTMA loading level, feed flow rate of HA, solution pH and optimum elution were investigated. The SMZ-75%, the flow rate of 2 BV/h and pH 10 were found to be optimum for the removal of HA. The elution using ethanol solution could regenerate SMZ effectively. It was found that the ethanol solution of 25% volume with the feed flow rate of 2 BV/h is sufficient to reduce HA concentration in the regeneration solution effluent to lower than 0.5 mg/L. The results of characterizations demonstrated that the most suitable orientation of the HDTMA adsorption on the zeolite surface is the formation of a hydrophobic organic monolayer. It is proposed that the hydrophobic nature of a HDTMA monolayer interacts favorably with the organic parts of HA, whereby the HA adsorption on SMZ surfaces is mainly due to the hydrophobic interaction, hydrogen bonding and partitioning mechanism.

Acknowledgements Thanks are due to the Ministry of Higher Education Malaysia for financial aid under GUP grant

(Q.J130000.7326.02J7) and to the Ministry of Higher Education Libya for scholarship to Awad F. Elsheikh.

Open Access This article is distributed under the terms of the Creative Commons Attribution 4.0 International License (<http://creativecommons.org/licenses/by/4.0/>), which permits unrestricted use, distribution, and reproduction in any medium, provided you give appropriate credit to the original author(s) and the source, provide a link to the Creative Commons license, and indicate if changes were made.

References

- Bajpai PK (1986) Synthesis of mordenite type Zeolite. *Zeolites* 6(1):2–8
- Castaldi P, Santona L, Enzo S, Melis P (2008) Sorption processes and XRD analysis of a natural zeolite exchanged with Pb^{2+} , Cd^{2+} and Zn^{2+} cations. *J Hazard Mater* 156(3–1):428–434
- Chen L, Wang TJ, Wu HX, Jin Y, Zhang Y, Dou XM (2011) Optimization of a Fe–Al–Ce nano-adsorbent granulation process that used spray coating in a fluidized bed for fluoride removal from drinking water. *Powder Technol* 206(3):291–296
- Childs CW (1994) Clay mineralogy—Spectroscopy and chemical determinative methods. In: Wilson MJ (ed) *Applied Clay Science*. Chapman and Hall, Hardcover, p 367
- Dabrowski A (1999) Adsorption—its development and application for practical purposes. In: Dabrowski A (ed) *Studies in surface science and catalysis*. Elsevier, pp 3–68
- Dabrowski A (2001) Adsorption—from theory to practice. *Adv Colloid Interface* 93(3–1):135–224
- Elaipoulos K, Perraki Th, Grigoropoulou E (2010) Monitoring the effect of hydrothermal treatments on the structure of a natural zeolite through a combined XRD, FTIR, XRF, SEM and N_2 -porosimetry analysis. *Microp Mesop Mater* 134(1–3):29–43
- Elsheikh AF, Ahmad UK and Ramli Z (2015) Removal of humic acid from water by adsorption onto dodecyltrimethylammonium bromide-modified zeolite in a fixed bed Reactor. *Desalin Water Treat* (1–17)
- Hsu Chen C, Ma Yi H (1988) Characterization of hydrophobic nature of high siliceous zeolite—sillalite by adsorption and diffusion. *Defense Technical Inform Center* 13:199–636
- Ismail AA, Mohamed RM, Ibrahim IA, Kini G, Koopman B (2010) Synthesis, optimization and characterization of zeolite A and its ion-exchange properties *Coll Surf A: Physicochem Eng Asp* 366(1–3):80–87
- Kim KJ, Ahn HG (2011) The effect of pore structure of zeolite on the adsorption of VOCs and their desorption properties by microwave heating. *Microp Mesop Mater* 152:78–83
- Lee J, Ha KT, Zoh KD (2009) Characteristics of trihalomethane (THM) production and associated health risk assessment in swimming pool waters treated with different disinfection methods. *Sci Total Environ* 407(6):1990–1997
- Lei C, Hu Y, He M (2013) Adsorption Characteristics of Triclosan from Aqueous Solution onto Cetylpyridinium Bromide (CPB) Modified Zeolites. *Chem Eng J* 219:361–370
- Leyva-Ramos R, Jacobo-Azuara A, Diaz-Flores PE, Guerrero Coronado RM, Mendoza-Barron J, Berber-Mendoza MS (2008) Adsorption of chromium(VI) from an aqueous solution on a surfactant-modified zeolite. *Colloid Surf* 330(1):35–41
- Li Z, Burt T, Bowman RS (2000) Sorption of ionizable organic solutes by surfactant-modified Zeolite. *Environ Sci Technol* 34(17):3756–3760

- Lin J, Zhan Y (2012) Adsorption of humic acid from aqueous solution onto unmodified and surfactant-modified chitosan/zeolite composites. *Chem Eng J* 200–202:202–213
- Matilainen A, Gjessing ET, Lahtinen T, Hed L, Bhatnagar A, Sillanpää M (2011) An overview of the methods used in the characterisation of natural organic matter (NOM) in relation to drinking water treatment. *Chemosphere* 83(11):1431–1442
- Mohd Omar F, Abdul Aziz H, Stoll S (2014) Aggregation and disaggregation of ZnO nanoparticles: influence of pH and adsorption of Suwannee river humic acid. *Sci Total Environ* 468–469:195–201
- Nakamoto H, Takahashi H (1982) Hydrophobic natures of zeolite ZSM-5. *Zeolites* 2(2):67–68
- Olson DH, Haag W, Haag W, Lago RM (1980) Chemical and physical properties of the ZSM-5 substitutional series. *J Catal* 61(2):390–396
- Qin Z, Shen B, Gao X, Lin F, Wang B, Xu C (2011) Mesoporous Y zeolite with homogeneous aluminum distribution obtained by sequential desilication and its performance in the catalytic cracking of cumene and 1,3,5 triisopropylbenzene. *J Catal* 278(2):266–275
- Rao P, Lo IMC, Yin K, Tang SCN (2011) Removal of natural organic matter by cationic hydrogel with magnetic properties. *J Environ Manage* 92(7):1690–1695
- Roger GM, Durand-Vidal S, Bernard O, Mériguet G, Altmann S, Turq P (2010) Characterization of humic substances and polyacrylic acid: a high precision conductimetry study. *Colloid Surface A* 356(1–3):51–57
- Rozic M, Ivanec Sipusic D, Sekovanic L, Miljanic S, Curkovic L, Hrenovic J (2009) Sorption phenomena of modification of clinoptilolite tuffs by surfactant cations. *J Coll Interf Sci* 331(2):295–301
- Shams K, Ahi H (2013) Synthesis of 5A zeolite nanocrystals using kaolin via nanoemulsion-ultrasonic technique and study of its sorption using a known kerosene cut. *Microp Mesop Mater* 180:61–70
- Shams K, Mirmohammadi SJ (2007) Preparation of 5A zeolite monolith granular extrudates using kaolin: investigation of the effect of binder on sieving/adsorption properties using a mixture of linear and branched paraffin hydrocarbons. *Microp Mesop Mater* 106(1–3):268–277
- Wang S, Peng Y (2010) Natural zeolites as effective adsorbents in water and wastewater treatment. *Chem Eng J* 156(1):11–24
- Wang S, Gong W, Liu X, Gao B, Yue Q (2006) Removal of fulvic acids using the surfactant modified zeolite in a fixed-bed reactor. *Separ Purif Tech* 51(3):367–373
- Yang J, Jia J, Liao J, Wang Y (2004) Removal of fulvic acid from water electrochemically using active carbon fiber electrode. *Water Res* 38(20):4353–4360
- Yang X, Shang C, Westerhoff P (2007) Factors affecting formation of haloacetonitriles, halo ketones, chloropicrin and cyanogen halides during chloramination. *Water Res* 41(6):1193–1200
- Zhan YH, Zhu ZL, Lin JW, Qiu YL, Zhao JF (2010) Removal of humic acid from aqueous solution by cetylpyridinium bromide modified zeolite. *J Environ Sci* 22(9):1327–1334
- Zhang WQ, Shi L, Tang KB, Liu ZP (2012) Synthesis, surface group modification of 3D MnV_2O_6 nanostructures and adsorption effect on Rhodamine B. *Mater Res Bull* 47(7):1725–1733